Electronic Supplementary Information for Dalton Transactions

Assembly of titanium embedded polyoxometalates with unprecedented structural features

*Thomas McGlone, Laia Vilà-Nadal, Haralampos N. Miras, De-Liang Long, Josep M. Poblet, and Leroy Cronin**

Supporting Information

Electrospray mass spectroscopic measurements

ESI measurements were made at 180 ºC. The solution of the sample, H_2O / CH_3CN (9:1), was diluted so that the maximum concentration of the cluster ions was of the order of 10^{-4} M and this was infused into the electrospray at 180 μL h^{-1}. The mass spectrometer used for the measurements was a Bruker microTOFQ and the data were collected in negative ion mode. The spectrometer was previously calibrated with the standard tune mix to give a precision of *ca.* 1.5 ppm in the region of 500–5000 *m*/*z*. The standard parameters for a medium mass data acquisition were used and the end plate voltage was set to −500 V and the capillary to +4500 V. The collision cell was set to a collision energy of −8.0 eV z^{-1} with a gas flow rate at 25 % of maximum and the cell RF was set at 1250 Vpp. The predicted spectrum is calculated using Bruker Data Analysis 3.4 and is performed by calculating the predicted distribution of the cluster anion. In Fig. 5, the spectrum is composed of $\{Ti_6(H_2O)_{10}(AsW^{VI}_7W^{V}O_{33})_2\}^{4-}$ and $\{Ti_6(H_2O)_{10}(HAsW^{VI}_7W^{V}O_{33})_2\}^{4-}$ which gives the formula weights for the di-anion of 1153.7 / 1154.2 compared to the observed *m*/*z* (100 %) peak which appears at 1153.6 / 1154.1 respectively.

Electrochemistry

Voltammograms were obtained using a Model Versastat 4 electro analysis system by Princeton Applied Research. The standard three-electrode arrangement was employed with a Pt mesh auxiliary electrode, 1.5 mm glassy carbon working electrode, and Ag / AgCl / KCl reference electrode at room temperature (19 ± 1 ^{o}C). All potentials are quoted relative to the Ag / AgCl / KCl reference electrode. The glassy carbon working electrodes (diameter 1.5 mm) were polished with alumina (3 μm) on polishing pads, rinsed with distilled water and sonicated in H_2O and then acetone solution before each experiment. The cell was purged with Ar for at least 10 min before each experiment.

The cyclic voltammetric behaviour of the solution was monitored for a 24 h period of time during which no voltammetric characteristics were changed. From our ESI-MS studies we know the compound retains its structural integrity in solution at room temperature as well as at higher temperatures, indicating that the compound is structurally stable under the experimental conditions we used. The Ti^{IV} and W^{VI} waves in the structure were not possible to be separated distinctly in CH_3CN nor in aqueous media. More specifically, Figs. S1 and S2 show the main characteristic peaks in the region -1.000 to +1.250 and -2.000 to 1.700 V of potential values vs Ag / AgCl at a scan rate of 100 mV s^{-1} in aqueous and organic solvent respectively. The form of the diagram remained identical no matter the scanning potential direction indicating that the phenomena observed in one domain had a negligible influence on those in the other domain. At the aforementioned scan rate and scanning towards the negative region of potential values, the reduction processes of the compound occur via two electrochemically irreversible steps, with the corresponding $E_{1/2}$ peak potentials located at -0.657 while in the case of the second redox couple it was not possible to determine the $E_{1/2}$ value since the process takes place close to the solvent's discharge limit. The oxidation peak though on the potential reversal is located at -0.842 V (vs. Ag / AgCl / KCl). As expected, no oxidation peaks were observed in the scanning from 0 V towards the positive region of potentials indicating that the initial oxidation state for the titanium centres is IV.

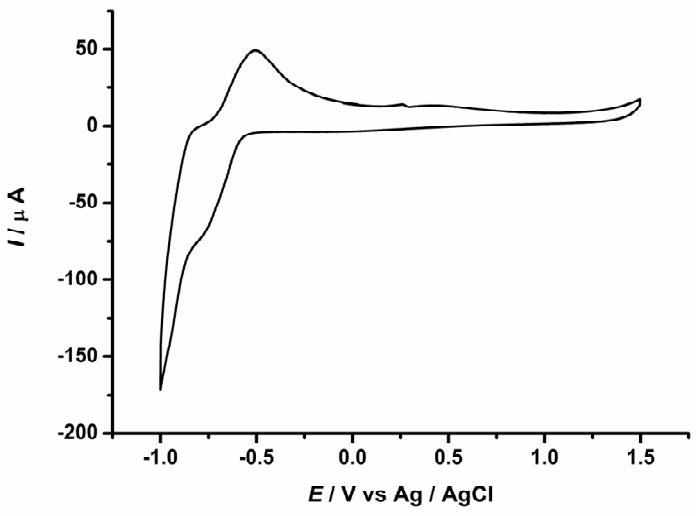

Fig. S1: Cyclic voltammograms of **2** (2×10^{-3} M) in aqueous 0.2 M Na_2SO_4 of 1 M CH_3COOH / CH_3COONa buffer solution. The scan rate was 100 mV s^{-1}, the working electrode was glassy carbon (1.5 mm) and the reference electrode was Ag / AgCl / KCl.

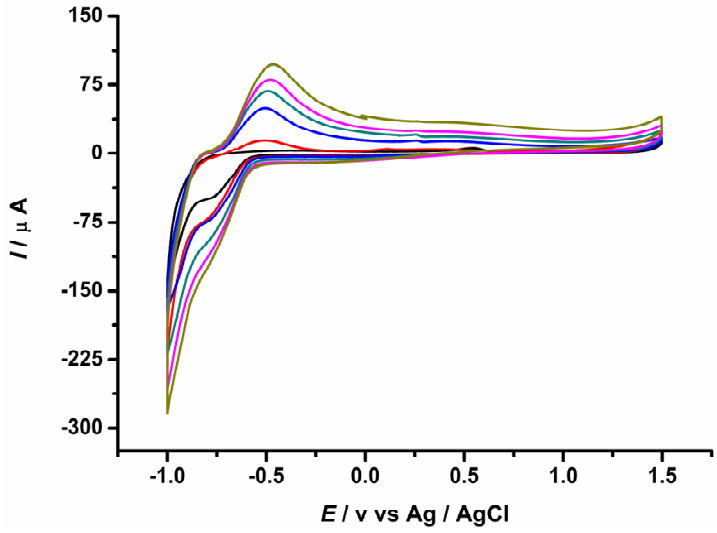

Fig. S2: Cyclic voltammograms of **2** at scan rates (from inner to outer) 25, 50, 100, 200, 300 and 400 mV/sec.

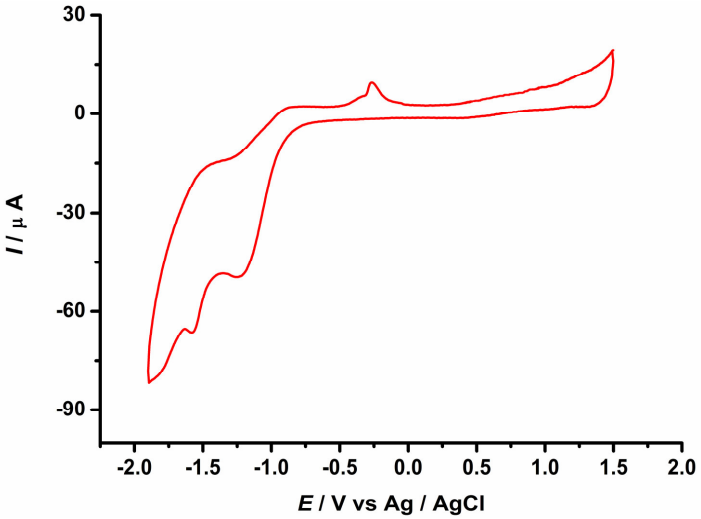

Fig. S3: Cyclic voltammograms of **TBA-2** (2×10^{-3} M) in 0.1 M $TBAClO_4$ of CH_3CN solution. The scan rate was 100 mV s^{-1}, the working electrode was glassy carbon (1.5 mm) and the reference electrode was Ag / AgCl / KCl.

Studying the electrochemical behaviour of **TBA-2** in CH_3CN, two well separated redox couples were observed similar to those observed in aqueous medium but shifted towards more negative values with the $E_{1/2}$ potential peaks observed at -1.059 and -1.525 V respectively. Additionally, an extra irreversible process observed at -0.300 V. In both cases, the form of the voltammograms as well as the location of the redox couples is in good agreement with previously reported Ti-substituted polyoxometalate species studied in aqueous[S1,S2,S3] and organic[S1,S4,S5] media respectively. Furthermore, the cyclic voltammograms of compound **2** in aqueous solution at different scan rates is represented in Fig. S2. The peak currents were proportional to the square root of the scan rate, indicating that the redox processes are diffusion-controlled in the 25 – 400 mV/sec region of scan rate. During the course of the studies in CH_3CN solution the redox peaks appeared to be significantly broadened at scan rate beyond 100 $mVsec^{-1}$ while at lower values of scan rate, passivation of the electrode's surface followed by broadening of the peaks took place which prevented us from collecting data of sufficient quality. The above mentioned behaviour has been observed and reported earlier in similar cases.[S1]

Themogravimmetric Analysis of Compounds 1, 2 and TBA-2

All materials were heated in a Pt pan under air at a rate of 10 ºC min^{-1} to 800 ºC.

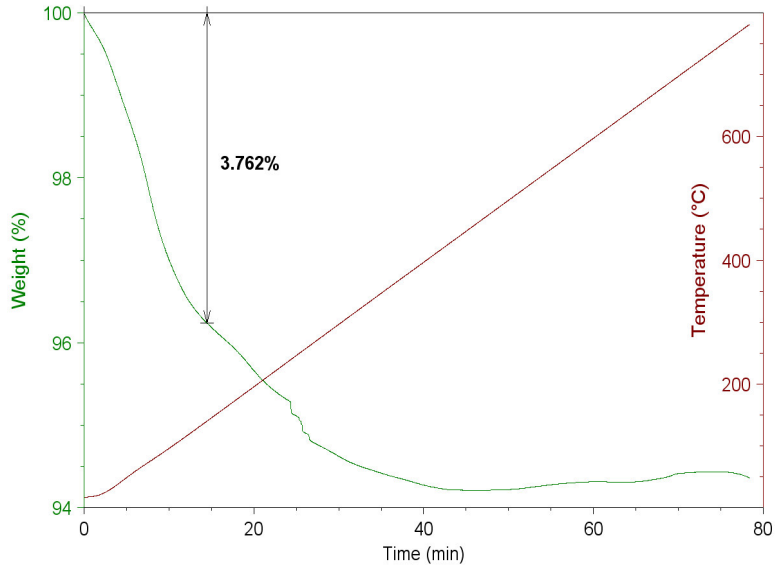

Fig. S4: TGA scan for compound **1**. The value of 3.76 % accounts for the loss of 11 water molecules (theoretical value 3.78 %). The number of solvent water molecules is much less than that in the formula deduced by crystallography due to the crystals losing water via exposure to the atmosphere. Further weight loss is observed as the cluster begins to decompose.

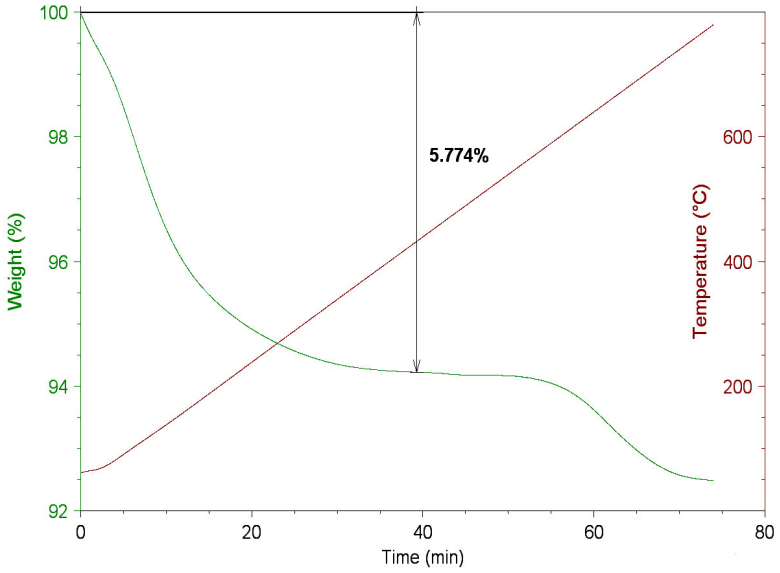

Fig. S5: TGA scan for compound **2**. The value of 5.77 % accounts for the loss of 10 aqua ligands and 6 solvent water molecules (theoretical value 5.81 %). Once again the number of solvent water molecules is much less than that in the formula deduced by crystallography due to the crystals losing water via exposure to the atmosphere. The decomposition temperature is much higher than that of **1**.

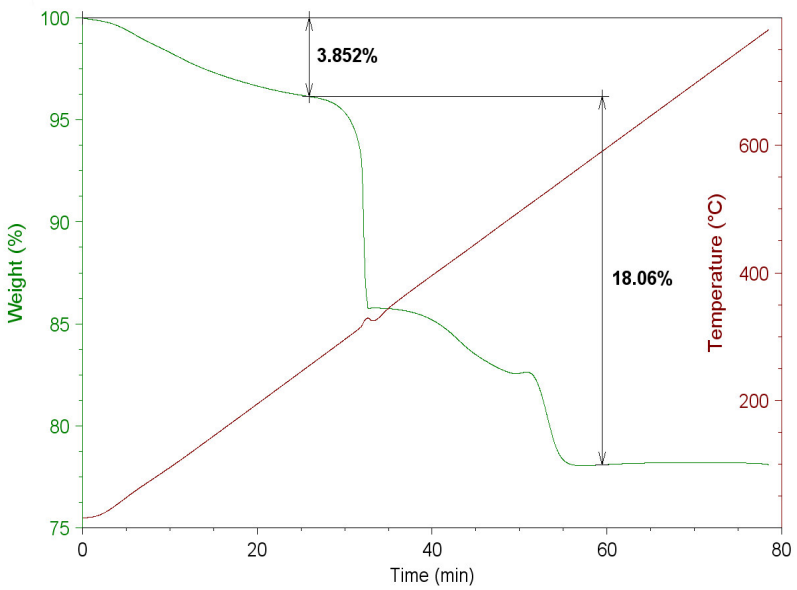

Fig. S6: TGA scan for compound **TBA-2**. The material was dried at 100 ºC beforehand to remove traces of Et_2O. The first weight loss is attributed to ten water molecules (theoretical value 3.22 %) due to the material absorbing air moisture and the second total weight loss is assigned to four TBA molecules (theoretical value 17.33 %).

FT-IR of Compounds 1 and 2

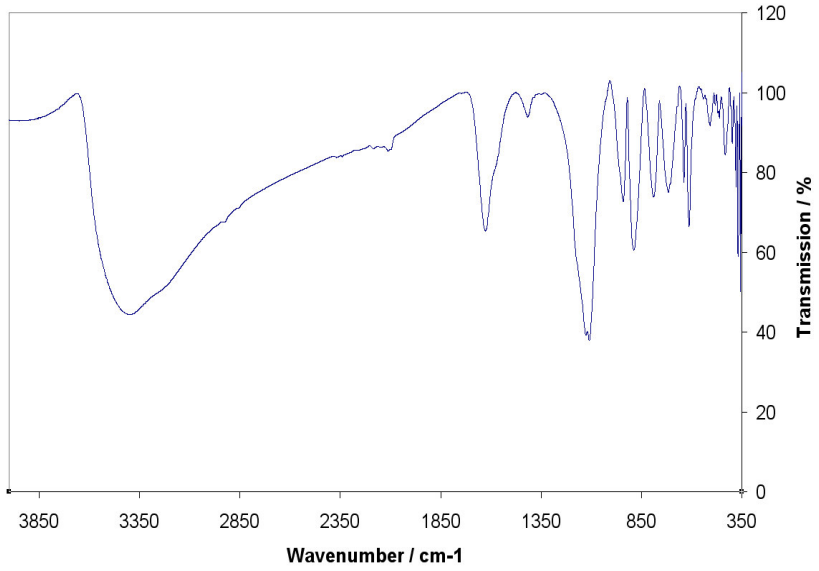

Fig. S7: FT-IR of compound **1**. FT-IR (KBr) characteristic IR-bands (in cm^{-1}); intensities denoted as vs = very strong, s = strong, m = medium, w = weak, vw = very weak, b = broad, sh = sharp: 3398 (s, br), 1627 (s, sh), 1415 (w, sh), 1110 (vs, sh), 941 (s, sh), 888 (s, sh), 790 (s, sh), 716 (s, sh), 638 (s, sh), 612 (s, sh), 507 (w, sh), 461 (vw, sh), 432 (m, sh), 397 (m, sh), 379 (s, sh), 369 (s, sh), 357 (vs, sh).

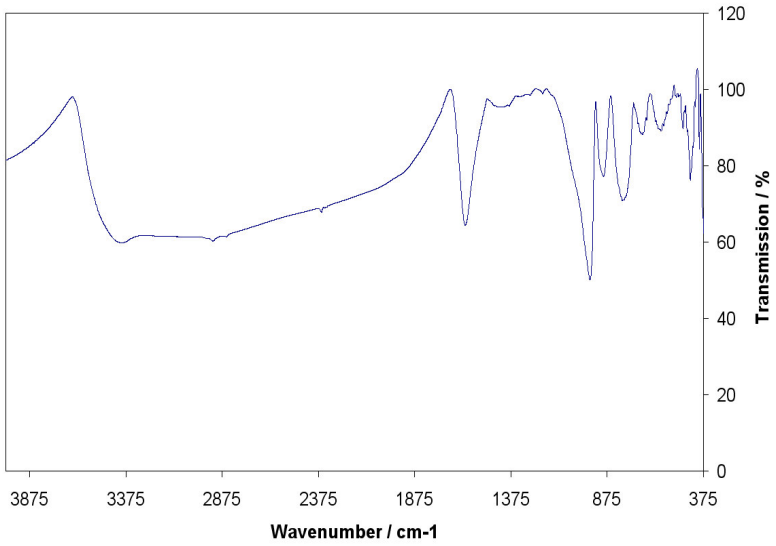

Fig. S8: FT-IR of compound **2**. FT-IR (KBr) characteristic IR-bands (in cm^{-1}); intensities denoted as vs = very strong, s = strong, m = medium, w = weak, vw = very

weak, b = broad, sh = sharp: 3399 (s, br), 1612 (s, sh), 964 (vs, sh), 895 (m, sh), 795 (s, sh), 692 (w, sh), 594 (w, sh), 481 (w, sh), 443 (m, sh), 396 (m, sh).

Density Functional Theory Calculations

The calculations were carried out by using DFT methodology with the ADF 2008 program. The gradient-corrected functionals of Becke and Perdew[44] for the exchange and correlation energies, respectively, were used to improve the description of the electronic density provided by the local density approximation. A set of Slater-type basis functions of triple-ζ + polarisation quality was employed to describe the valence electrons of all the atoms. Frozen cores consisting of the 1s shell for O and Na, the 1s to 4d shells for W, the 1s to 2p shells for Ti, the 1s to 4p shells for Sb, the 1s to 3p shells for As were described by means of single Slater functions. Scalar relativistic corrections were included by means of the zeroth-order regular approximation (ZORA) formalism. The BP86 / TZP calculations have been proven to be a very adequate methodology to study the electronic structure of polyoxometalates (J. A. Fernandez, X. Lopez, C., Bo, C. de Graaf, E. J. Baerends, J. M. Poblet, *J. Am. Chem. Soc.* **2007,** 129, 12244; X. Lopez, I. A. Weinstock, C. Bo, J. P. Sarasa, J. M. Poblet, *Inorg. Chem.* **2006,** 45, 6467; J. M. Poblet, X. Lopez, C. Bo, *Chem. Soc. Rev.* **2003,** 32, 297). All the computed stationary points have closed-shell electronic structure. All the structures discussed through this work were optimised in the presence of a continuous model solvent by means of the conductor-like screening model (COSMO) implemented in the ADF code (C. C. Pye, T. Ziegler, *Theor. Chem. Acc.* **1999,** 101, 396). To define the cavity that surrounds the molecules we use the solvent accessible surface (SES) method and a fine tesserae. The ionic radii of the atoms, which define the dimensions of the cavity surrounding the molecule, are chosen to be (in Å) 1.26 for W, 1.52 for O, 1.20 for H, 0.655 for Ti, 0.725 for Sb, 0.56 for As and 1.36 for Na. The dielectric constant is set to 78 so as to model water as solvent.

Compound **1**: $[TiO(SbW_9O_{33})_2]^{16-}$

The compound $\{[TiO(SbW_9O_{33})_2]\}^{16-}$ has a high negative charge and proved difficult to reproduce in the calculations. To overcome this we have optimised two structures with 3 and 5 Na atoms, hence reducing the charge. However the charge remains high and must be stabilised by solvent water molecules. We have used COSMO to model

this and also applied symmetry considering a global C_{2v} arrangement, with a C_2 axis on the Ti-Oa bond, see Fig. S9.

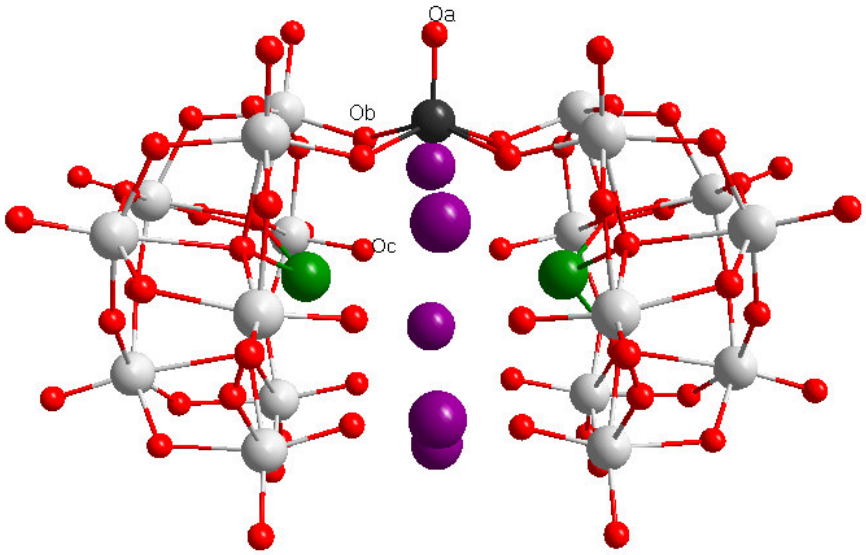

Fig. S9: The optimised $\{Na_5[TiO(SbW_9O_{33})_2]\}^{11-}$ structure. W: grey, Sb: green, Na: purple, Ti: black, O: red.

		Symmetry C2v	
Distance (Å)	Experimental $[TiO(SbW_9O_{33})_2]^{16-}$	Calculated (5Na) $\{Na_5[TiO(SbW_9O_{33})_2]\}^{11-}$	Calculated (3Na) $\{Na_3[TiO(SbW_9O_{33})_2\}^{13-}$
Ti-Oa	1.653(9)	1.67	1.67
Ti-Ob	1.998(8) 2.000(8) 1.989(8) 1.952(7) *Mean* = 1.986	2.02	2.02
Ti-Oc	1.741 1.756 1.750 1.750 1.753 1.744 1.711 1.756 *Mean* = 1.745	1.79	1.78
Sb-Sb	5.134	5.27	5.48

Fig. S10: Table with experimental and optimised distances for $[TiO(SbW_9O_{33})_2]^{16-}$

Using these calculations we have reproduced experimental values for the bonds. The geometry with 5 Na cations gives the best approximation to the X-ray structure,

suggesting that these atoms provide extra stabilisation to the compound. Reducing the number of Na atoms results in an increase in Sb-Sb distance of 0.21 Å.

Having successfully optimised the structure with five central Na cations, we also carried out some calculations with hydrogen atoms.

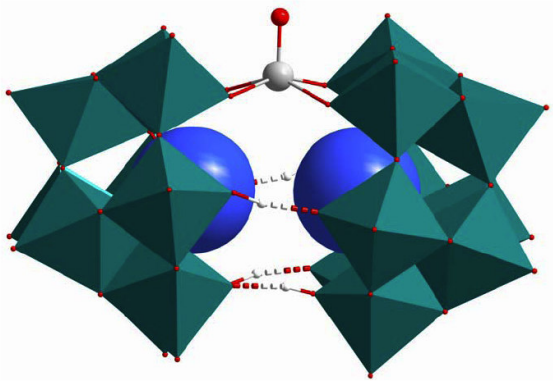

Fig. S11: Optimised structure with four protons $\{TiO(H_2SbW_9O_{33})_2)\}^{12-}$. Surrounding Na cations have been omitted in the calculation. W: teal polyhedra, Sb: blue, Ti: grey, O: red.

The negative charge of $\{TiO(SbW_9O_{33})_2\}^{16-}$ has now been reduced by 4 protons added to four terminal W=O bonds. The calculation of $[TiO(H_2SbW_9O_{33})_2]^{12-}$ has been performed using COSMO to model solvent water without symmetry constraints. The results show that in acidic solution the terminal oxygens could be protonated to some extent and hence the negative charge would be compensated by protons rather than Na cations. However since the solution is in a dynamic environment, both protons and Na cations could be present in the inner part of the molecule.

Compound **2**: $[Ti_4(H_2O)_{10}(AsTiW_8O_{33})_2]^{6-}$

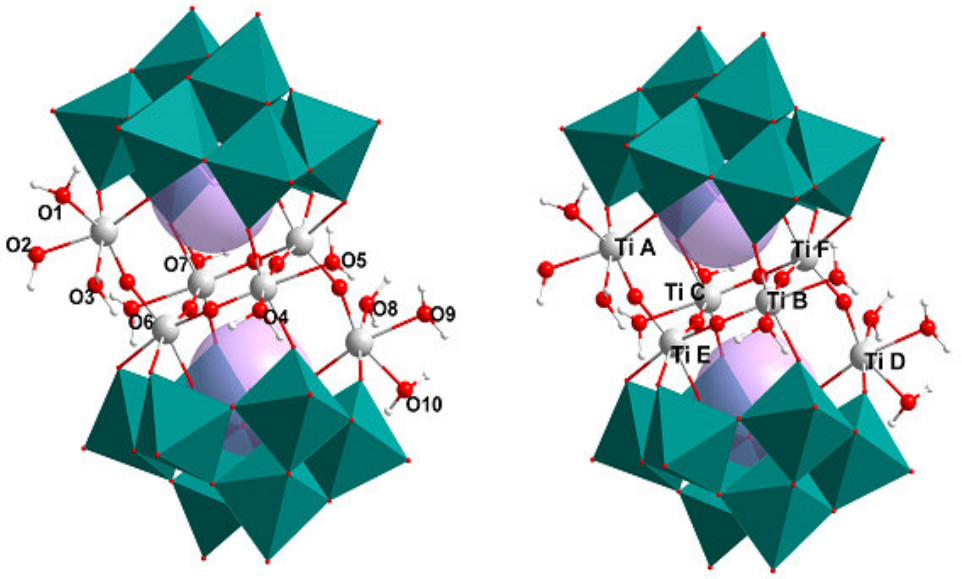

Fig. S12: Optimised structure of $[Ti_4(H_2O)_{10}(AsTiW_8O_{33})_2]^{6-}$ with labelled oxygen atoms (left) and titanium atoms (right). W; teal polyhedra, Ti: grey, As: pink, O: red, H: white.

The inclusion of 10 H_2O molecules in the optimisation utilised a great computational effort and the result of the calculation featured a good experimental match, see Fig. S13. In general modelling polyoxoanions with water ligands is always a non trivial task.

Distance (Å)	Experimental	Theoretical	|Exp-Calc| (Å)
As–As	6.044	6.059	0.014
Ti_A–Ti_D	9.508	9.381	0.127
Ti_C–Ti_E	3.639	3.629	0.010
Ti_E–Ti_B	3.615	3.549	0.067
Ti_B–Ti_F	3.639	3.655	0.016
Ti_F–Ti_C	3.615	3.554	0.061
Ti_A–O–Ti_E	1.806(6)	1.805	0.001
Ti_D–O–Ti_F	1.806(6)	1.810	0.004
Ti_B–O–Ti	1.790(6), 1.798(6)	1.784, 1.805	0.006, 0.007
Ti_C–O–Ti	1.790(6), 1.798(6)	1.783, 1.804	0.007, 0.006
Ti_A–O–W	1.823(6), 1.847(5)	1.820, 1.824	0.003, 0.023
Ti_D–O–W	1.823(6), 1.847(5)	1.828, 1.822	0.005, 0.025
Ti_B–O–W	1.932(6), 1.954(5)	1.964, 1.937	0.032, 0.017
Ti_C–O–W	1.932(6), 1.954(5)	1.978, 1.952	0.046, 0.002

Fig. S13: Table showing experimental and theoretical distances (in Å) for several representative atoms in the $[Ti_4(H_2O)_{10}(AsTiW_8O_{33})_2]^{6-}$ structure.

Oxygen in H_2O	Distance Ti-OH_2 (Å)		|Exp.-Calc.| (Å)
	Experimental	Theoretical	
O1	2.142(6)	2.228	0.09
O2	2.096(7)	2.241	0.15
O3	2.179(7)	2.291	0.11
O4	2.206(6)	2.360	0.15
O5	2.185(6)	2.333	0.15
O6	2.185(6)	2.343	0.16
O7	2.206(6)	2.314	0.11
O8	2.179(7)	2.276	0.10
O9	2.096(7)	2.230	0.13
O10	2.142(6)	2.246	0.10

Fig. S14: Table showing experimental and theoretical distances (in Å) for Ti-OH_2 bonds and the absolute values of the differences between both.

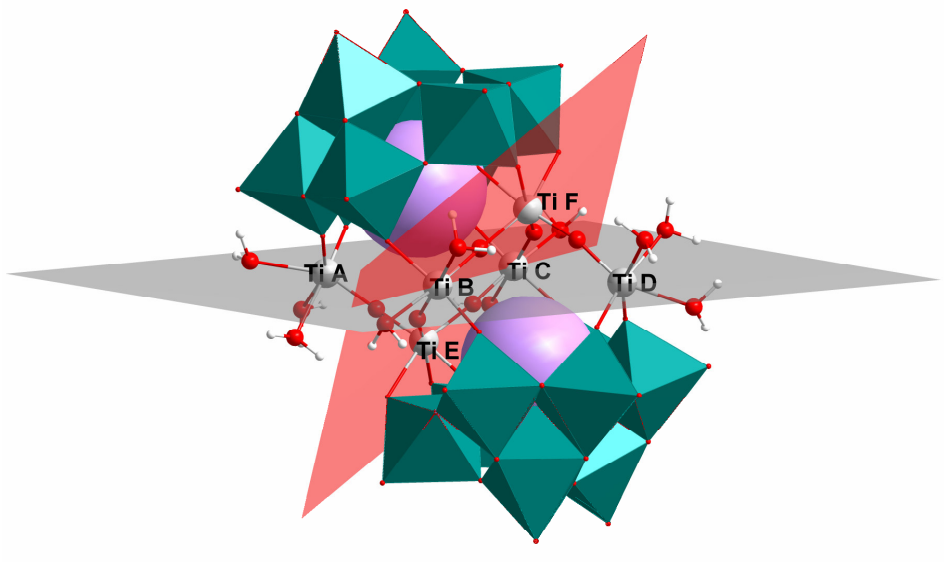

Fig. S15: Optimised structure of $[Ti_4(H_2O)_{10}(AsTiW_8O_{33})_2]^{6-}$ showing the two planes containing the six Ti atoms. Grey plane: Ti_A, Ti_B, Ti_C and Ti_D. Red plane: Ti_E, Ti_B, Ti_C and Ti_F.

Catalytic Experiments

Oxidation of Benzyl Alcohol to Benzaldehyde

30.0 mg (5586.71 $gmol^{-1}$, 5.37 μmol) of $(TBA)_4H_2[(AsTiW_8O_{33})_2Ti_4(H_2O)_{10}]$ **TBA-2** was dissolved in 5 ml of CD_3CN. 80 μL of benzyl alcohol (d_c = 1.04 gml^{-1}, 0.768 mmol) was added, followed by 40 μL H_2O_2 (30 %), and the mixture was heated to 60 ºC. ^1H NMR spectra were measured at time t = 0, 1 h, 2 h and 3 h.

The presence of the protons from the TBA cations can be clearly assigned in the ^1H NMR spectra and are used to verify the integrations during the catalytic experiment. The aromatic protons on the phenyl ring of benzyl alcohol (7.0 – 7.5 ppm) and those from the $–CH_2-$ group (4.64 ppm) are also easily identifiable. Due to the presence of water in the H_2O_2 solution used, a broadened signal (2.5 – 3.0 ppm) arises due to some overlapping with one group of protons on the TBA cations.

While some new peaks appear in the range of 7.5 to 8.0 ppm, the signal at 10 ppm from the benzaldehyde proton can be observed and calculations based on the relative intensity of signals at 10 ppm and 4.64 ppm show the conversion levels of benzyl alcohol.

It is noteworthy that for the 3 hrs reaction time, there is absolutely no indication of benzyl alcohol oxidation in an identical system with no catalyst.

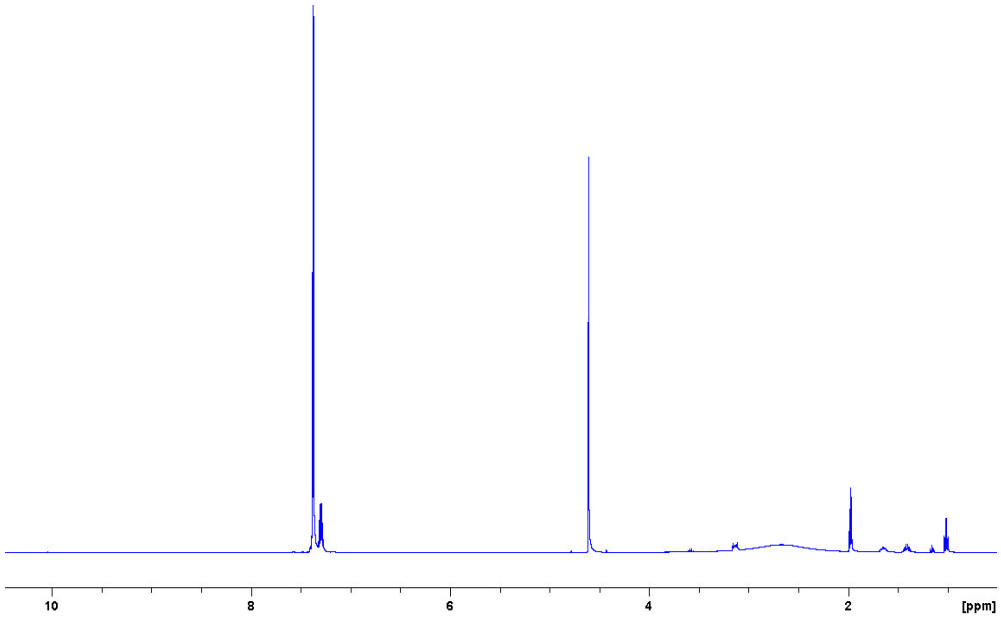

Fig. S16: t = 0, with 0 % conversion.

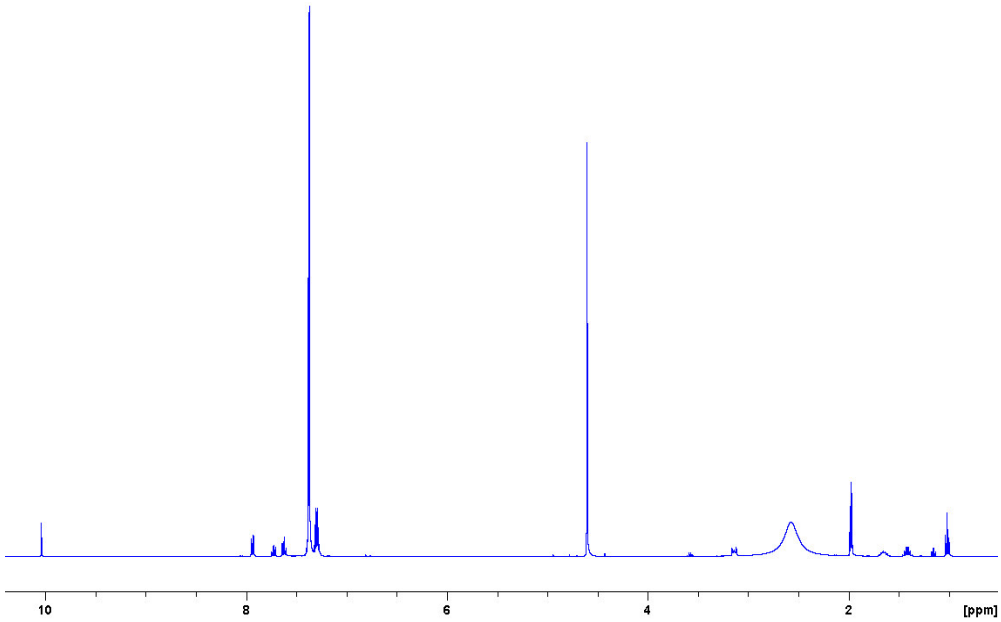

Fig. S17: t = 1 h, with 6.8 % conversion.

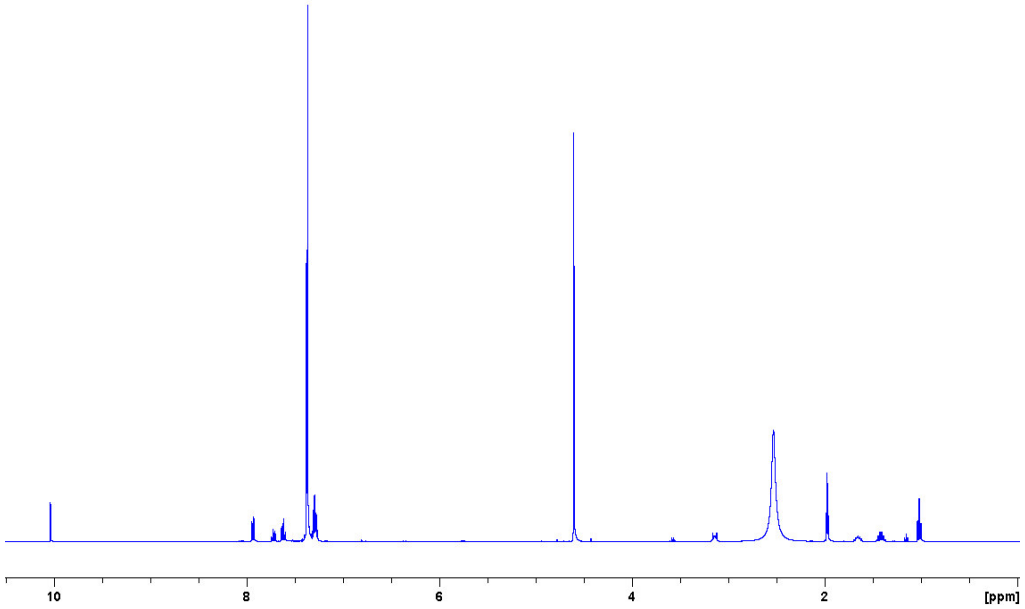

Fig. S18: t = 2 h, with 8.1 % conversion.

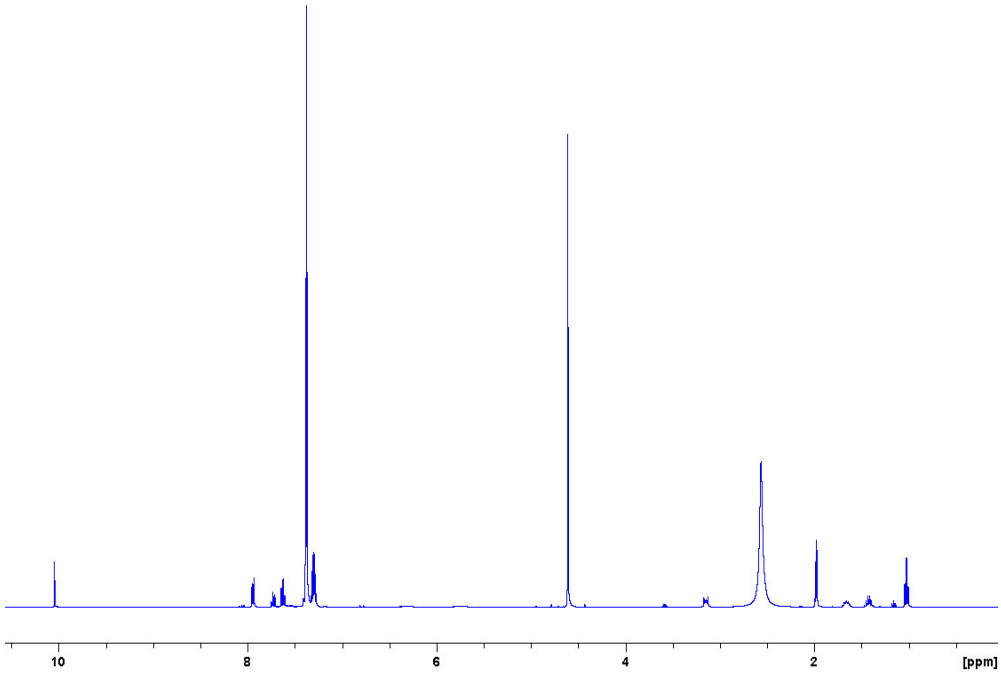

Fig. S19: t = 3 h, with 8.3 % conversion.

Literature

[S1] F. Hussain, B. S. Bassil, U. Kortz, O. A. Kholdeeva, M. N. Timofeeva, P. de Oliveira, B. Keita and L. Nadjo, *Chem. Eur. J.* 2007, **13**, 4733-4742.

[S2] O. A. Kholdeeva, G. M. Maksimov, R. I. Maksimovskaya, L. A. Kovaleva, M. A. Fedotov, V. A. Grigoriev and C. L. Hill, *Inorg. Chem.* 2000, **39**, 3828-3837.

[S3] O. A. Kholdeeva, T. A. Trubitsina, R. I. Maksimovskaya, A. V. Golovin, W. A. Neiwert, B. A. Kolesov, X. Lopez and J. M. Poblet, *Inorg. Chem.* 2004, **43**, 2284-2292.

[S4] R. Murugesan, P. Sami, T. Jeyabalan and A. Shunmugasundaram, *Proc. Indian Academy Sci.-Chem. Sci.* 1995, **107**, 1-10.

[S5] R. Murugesan, P. Sami, T. Jeyabalan and A. Shunmugasundaram, *Trans. Metal Chem.* 1998, **23**, 583-588.